ORIGINAL ARTICLE

Hedgehog signalling pathway activation in gastrointestinal stromal tumours is mediated by primary cilia

Pablo Iruzubieta[1,3] · Marta Monzón[1] · Tomás Castiella[2,3] · Teresa Ramírez[2] · Concepción Junquera[1,3]

Abstract

Background Gastrointestinal stromal tumour (GIST) is a mesenchymal cancer which derives from interstitial cells of Cajal. To determine whether a relationship between Hedgehog (Hh) signalling pathway and primary cilia exists in GIST tumours is intended here.

Methods Immunohistochemical, immunofluorescence and ultrastructural techniques were performed in this study.

Results We show that GIST cells present primary cilia (an antenna-like structure based on microtubules). But, moreover, we prove Hedgehog signalling pathway activation in these tumours (a pathway related with tumoural features such as proliferation, migration or stemness) and we show for the first time that this signalling pathway activation in GIST is mediated by primary cilia, likely in a paracrine way.

Conclusion Thus, primary cilia and Hedgehog signalling would be fundamental in tumoural microenvironment control of GIST cells for their maintenance, differentiation and proliferation.

Keywords GIST · Primary cilium · Hedgehog signalling · Ultrastructure · Immunohistochemistry

Introduction

Gastrointestinal stromal tumour (GIST) is the most common mesenchymal neoplasm of the human gastrointestinal tract. Incidence rates of GIST range between 6.5 and 14.5 per million per year [1]. It is mostly located in the stomach (60%) followed by the jejunum and ileum (30%), the duodenum (5%), colorectum (4%) and oesophagus or appendix (< 1%) [2]. On the basis of immunophenotypical and ultrastructural similarities [3, 4], these tumours are thought to derive from Interstitial Cells of Cajal (ICCs) or an ICC progenitor through somatic mutation.

GISTs have been classically classified into three principal subtypes attending to their morphology. According to published data, approximately 70% of cases are composed of spindle cells characterised by ovoid nuclei, paranuclear vacuolisation and syncytial cell borders. Around 20% of GISTs show epithelioid cells with round nuclei and the remaining 10% of cases show both mixed cellular populations [2].

Gain-of-function mutations in *KIT* are found in 70–80% of GISTs whereas *PDGFRA* tyrosine kinase receptor mutations are present in 10–15% of cases [3, 5]. Recently, ANO1, also known as TMEM16A or DOG1, has been reported as a highly sensitive and specific marker of GIST [6] irrespective of *KIT* or *PDGFRA* mutations [7]. It may stain up to one-third of KIT-negative GIST [8]. Thus, ANO1 has been proposed to be included in routine studies of GIST [9]. ANO1 is a calcium-activated chloride channel; it has been showed to regulate proliferation in ICCs [10] and primary ciliogenesis [11]. However, its exact role in GISTs remains elusive [12, 13].

Primary cilia are non-motile organelles composed by an axoneme of 9 peripheral doublets of microtubules (9 + 0 structure) projecting out of the cell surface. The axoneme

✉ Pablo Iruzubieta
pablo.iruzubieta@hotmail.es

1 Department of Human Anatomy and Histology, Faculty of Medicine, University of Zaragoza, Zaragoza, Spain

2 Department of Pathological Anatomy, Legal and Forensic Medicine and Toxicology, Faculty of Medicine, University of Zaragoza, Zaragoza, Spain

3 Institute for Health Research Aragón (IIS), C/Domingo Miral s/n, 50009 Zaragoza, Spain

is originated from a basal body composed by a modified centriole that is anchored to the cell membrane by the transition fibres [14]. The transition zone, located between the axoneme and the basal body, acts as a gate that controls the traffic of proteins and lipids providing primary cilia with a different composition from cytosol and plasma membrane [15]. Primary cilia have important functions in different tissues based on three relevant features: supply of cell polarity, regulation of cell cycle and acting as sensory antenna for cell signalling [16]. Thus, several signalling pathways (such as Hedgehog, Wnt or TGFβ) have been identified as primary cilia dependent [17, 18]. Moreover, mutations in primary cilia are related to a group of disorders called ciliopathies [16, 19].

In addition, primary cilia involvement in cancer has been closely related to the Hedgehog (Hh) signalling pathway [20, 21]. Hence, Hh signalling pathway activates transcription of different genes related to processes impaired in tumours such as cell proliferation, apoptosis, angiogenesis or epithelial–mesenchymal transition [22]. Furthermore, Hh signalling pathway has been recently implicated in maintenance and proliferation of cancer stem cells [21]. In fact, abnormal activation of this signalling pathway (both in a ligand-dependent and -independent way) can lead to cancer [20, 22].

Three Hh ligands have been identified in vertebrates: Indian (Ihh), Desert (Dhh) and Sonic (Shh). When the pathway is not activated, the Patched receptor is located in the ciliary membrane repressing the G-protein-coupled Smoothened (Smo) receptor by preventing its trafficking and localisation to ciliary membrane [20, 22, 23]. Then, Gli1 transcription factor is sequestered by SUFU while Gli2 and Gli3 are converted into their repressor forms [23]. Conversely, when the Hh ligands bind Patched, it is removed out from the primary cilia axoneme facilitating Smo localisation in ciliary membrane [24]. Smo produces SUFU-Gli1 dissociation, allowing Gli1 to enter the nucleus and activate gene transcription [18, 23].

Although previous studies have already identified the Hh signalling pathway in GIST [25, 26], here we evidence for the first time its activation by primary cilia in this type of tumours.

Materials and methods

Materials

Eight cases of stomach tumours that fulfilled the histological criteria of GISTs were examined in this study. Four of them were low-grade GIST, while the remaining four were high grade. They were retrieved from the files of the Department of Pathology at the University Clinic Hospital of Zaragoza.

All protocols developed were approved by the Human Research Ethics Committee (*Comité Ético de Investigación Clínica de Aragón, CEICA*) from the *Instituto Aragonés de Ciencias de la Salud* (IACS).

Immunohistochemistry

Immunohistochemical staining was performed on 2-μm-thick formalin-fixed paraffin-embedded sections using EnVision® (DAKO) method. The primary antibodies used in this study were: polyclonal rabbit anti-KIT (1:50, A4502 DAKO; Glostrup, Denmark), polyclonal rabbit anti-ANO1 (1:100, Abcam, ab53212; Cambridge, UK), polyclonal rabbit anti-Gli1 (1:200, Abcam, ab49314; Cambridge, UK), polyclonal rabbit anti-Smo (1:1000, LS Bioscience, LS-B4911, Seattle, WA, USA) and polyclonal goat anti-Patched (1:100, Santa Cruz, sc-6149; Dallas, TX, USA). Antibodies were diluted with DAKO diluent (S2022). The tissue sections were deparaffinised in xylene for 20 min and rehydrated in graded ethanol (4 min in 100°, 4 min in 96°, 4 min in 70° and 5 min in distilled water). Prior to all assays, a heat-induced antigen retrieval step was performed for KIT, ANO1, Gli1 and Smo immunolabeling using buffer citrate (pH 6, DAKO S2031) by treatment for 5 min in microwave at 800 W and 3 additional minutes at 360 W. For Patched staining, an antigen retrieval step using Tris-buffered saline (TBS, pH 9) was performed at 96 °C for 20 min.

After washing twice with PBS for 3 min, endogenous peroxidase was blocked using peroxidase blocking reagent (DAKO, S2001) for 10 min and sections were washed in distilled water and PBS 3 min, twice.

Afterwards, sections were incubated with primary antibodies at 4 °C overnight in a humidified chamber. Sections were washed in PBS three times for 5 min and incubated with Labelled Polymer EnVision-HRP (DAKO K5007) or Polyclonal Rabbit Anti-Goat Immunoglobulins/HRP (1:200, DAKO, P016002-2) for 1 h. To confirm the presence of immunocomplexes, 3,3′-diaminobenzidine as chromogen and hydrogen peroxide as substrate were used. The samples were washed twice in distilled water, contrasted with Mayer's haematoxylin for 7 min, washed in tap water for 15 min, dehydrated in a graded ethanol (2 min in 70°, 2 min in 96° and 5 min in 100°), cleared in xylene and cover slipped with Eukitt (03989 Sigma-Aldrich; St. Louis, MO, USA).

Digital images were captured by Olympus BX1 microscope.

Immunofluorescence microscopy

Two-micrometre formalin-fixed paraffin-embedded sections were cut and mounted on glass slides. The sections were deparaffinised in xylene for 20 min and rehydrated in graded ethanol (4 min in 100°, 4 min in 96°, 4 min in 70°

and 5 min in distilled water). Tissues were permeabilised with 0.1% Triton X-100 in PBS for 8 min. Afterwards an antigen retrieval step using Tris-buffered saline (TBS, pH 9) was performed at 96 °C for 20 min for Acetylated-tubulin, Pericentrin and Patched. For Gli1 unmasking, a protocol using buffer citrate (pH 6, DAKO S2031) and treatment for 5 min in microwave at 800 W and 3 additional minutes at 360 W was used.

Sections were incubated overnight at 4 °C with the following primary antibodies: monoclonal mouse anti-Acetylated-tubulin (1:4000, Sigma Aldrich, T7451; St. Louis, MO, USA), polyclonal rabbit anti-Pericentrin (1:100, Abcam, ab4448; Cambridge, UK), polyclonal goat anti-Patched (1:100, Santa Cruz, sc-6149; Dallas, TX, USA) and polyclonal rabbit anti-Gli1 (1:200, Abcam, ab49314; Cambridge, UK) in a dark humidified chamber. Sections were washed in PBS three times for 5 min and incubated for 1 h at RT in a dark humidified chamber with secondary antibodies: donkey anti-mouse IgG H+L Alexa Fluor 594 (1:1000, ThermoFisher, R37115; Waltham, MA, USA), donkey anti-rabbit IgG H+L Alexa Fluor 488 (1:1000, ThermoFisher, A-21206; Waltham, MA, USA) and donkey anti-goat IgG H+L Alexa Fluor 488 (1:1000, ThermoFisher, A-11055; Waltham, MA, USA). After washing in PBS, DAPI (1 µg/mL, Sigma-Aldrich) was added for 1 min for nuclei counterstaining. Sections were washed in PBS and the slides were covered with fluorescence mounting medium (DAKO, S3023).

Samples were visualised with a fluorescence microscope (Olympus BX1 with DP70 Digital Camera System) and analysed with DP Controller Software. Every fluorescent channel was individually photographed and channels were merged using FIJI Image_J software [27].

Electron microscopy

After tumour extraction, samples (about 1–1.5 mm^3) were washed in phosphate buffer and fixed with 2.5% glutaraldehyde and 2% paraformaldehyde overnight at RT, washed in 0.1 M phosphate buffer for 5 min, post-fixed with 2% osmium, rinsed, dehydrated in graded acetone (30%, 50%, 70% with 2% uranyl acetate, 90%, 100%), cleared in propylene oxide and embedded in araldite (Durcupan, Fluka AG; Buchs SG, Switzerland).

Semi-thin sections (1.5 µm) were cut with a diamond knife, lightly stained with 1% toluidine blue and examined by light microscopy (Olympus BX51 microscope, Olympus Imaging Corporation; Tokyo, Japan). Later, ultrathin (0.05 µm) sections were cut, collected on Formvar-coated single-slot grids counterstained with 1% uranyl acetate and Reynold's lead citrate for 10 min.

They were examined under a FEI Tecnai G2 Spirit TEM. The images were captured with Advanced Microscopy Techniques, using a Corp. Charge-Coupled Device imaging system (CCD from Danvers, MA, USA).

Three-dimensional reconstructions from serial electron microscopy sections were performed using FIJI Image J software [27].

Results

GIST histological study

Haematoxylin–eosin studies showed two cell populations in the studied samples: on the one hand, spindle cells with ovoid nuclei and the characteristic paranuclear vacuoles (Fig. 1a, b); on the other hand, epithelioid cells with round nuclei and pale cytoplasm. Spindle cells were generally more numerous than epithelioid.

Moreover, we performed immunohistochemical experiments to confirm the diagnosis of GIST through the well-known GIST markers: KIT (Fig. 1c) and ANO1 (Fig. 1d). Both markers were positive in all samples, showing a cytoplasmic staining.

Thus, we identified our samples as GIST tumours, showing predominantly spindle cells and expressing both KIT and ANO1.

Primary cilia in GISTs

We performed double immunofluorescence experiments to co-localise Acetylated-tubulin (specific to axoneme of cilia) and Pericentrin (present in centrioles, including the basal body of cilia) (Fig. 2). Hence, a substantial number of GIST cells were evidenced to present primary cilia in determined areas from an overview picture (Fig. 2a–c).

Quantitative analyses were performed by counting the number of ciliated cells per High Power Field (HPF, magnification 400×) in areas of GIST samples where immunofluorescence staining was mainly positive. Thus, we showed that up to 25% of total cells were ciliated (Fig. 2d), discarding primary cilium as an occasional finding in GIST cells.

These primary cilia were also studied at ultrastructural level using Transmission Electron Microscopy (TEM). Primary cilia components (including basal body, transition zone and axoneme) were clearly identified (Fig. 3a–c) and active vesicular trafficking through the basal body was showed (Fig. 3d), confirming the dynamic nature of this organelle. Moreover, primary cilium is showed here projecting out of GIST cells and directly protruding into neighbour cell cytoplasm (Fig. 4a, b).

Furthermore, serial sections for TEM were performed with the purpose of reconstructing the three-dimensional disposition of primary cilium in GISTs (Fig. 4c, Online Resource 1). These reconstructions helped to clarify the
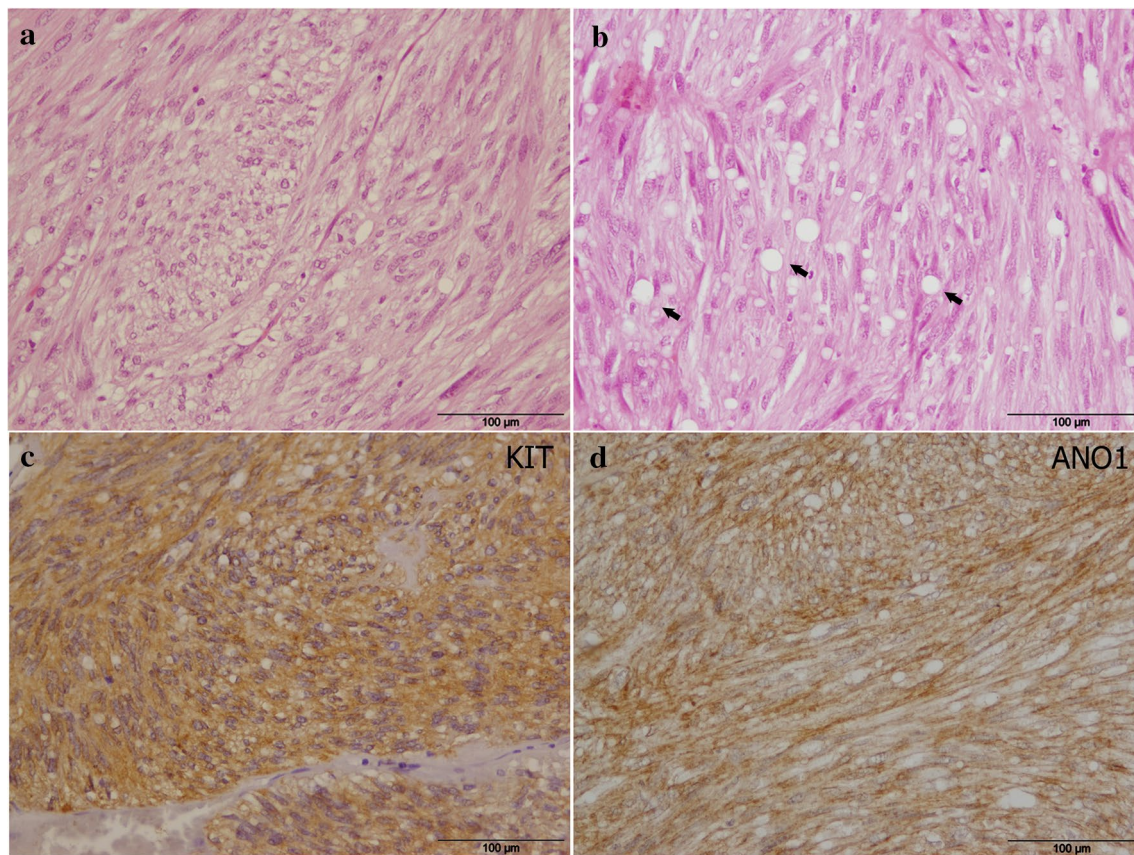
Fig. 1 GIST general histological study. **a** Spindle (sp) cells were predominant in GIST tumours. **b** These cells were characterised by ovoid nuclei and a prominent paranuclear vacuole (arrows). **c** GISTs showed homogeneous cytoplasmic staining for KIT. **d** Specific immunostaining for ANO1 was also evidenced in cancer cells

disposition of ciliary components, their relation with cellular organelles (as Golgi apparatus or mitochondria) and the physical contacts that they mediate between neighbouring cells.

Hh signalling pathway in GISTs

To elucidate the role of primary cilia in GISTs, Hh signalling pathway and the relation of this signalling cascade with primary cilia in these cells were assessed. Thus, immunolabelling techniques for Patched, receptor of Hh ligands that trigger the activation of the pathway; Smo, which activates Gli1 nuclear translocation after entering primary cilia axoneme, and Gli1, the main effector transcription factor of the cascade were applied.

Immunolabelling studies for Patched evidenced a punctiform staining frequently located next to nuclei (Fig. 5a). With the aim of clarifying the relation of Hh signalling pathway with primary cilia, co-localisation studies for Acetylated-tubulin (as a marker for primary cilia) and Patched

were developed. We found that Patched was not located in ciliary axoneme but it was concentrated in ciliary basal body (Fig. 5b). This localisation in basal body suggests the activation of Hh signalling pathway through binding of Hh ligands to Patched receptor and its internalisation and removal from the axoneme of cilia. Furthermore, we showed Smo expression in cell membrane and regions near to nuclei (Fig. 6), suggestive of Hh signalling pathway activation.

Specific Gli1 immunostaining was detected in cytoplasm and nucleus of some cells (Fig. 7a, b). Gli1 presence in nuclei gives evidence of the activation of Hh pathway in GIST cells. Moreover, we performed immunofluorescence experiments to show the presence of primary cilia in Gli1 + cells. Our results showed that cells with primary cilia showed Gli1 expression in nuclei, confirming the Hh activation in ciliated cells (Fig. 7c).

Thus, Hh signalling pathway would be activated in GIST cells through primary cilia producing Patched removal from cilia axoneme, Smo entrance to axoneme and consequent Gli1 activation and transportation to nucleus, where transcription of target genes is switched on.
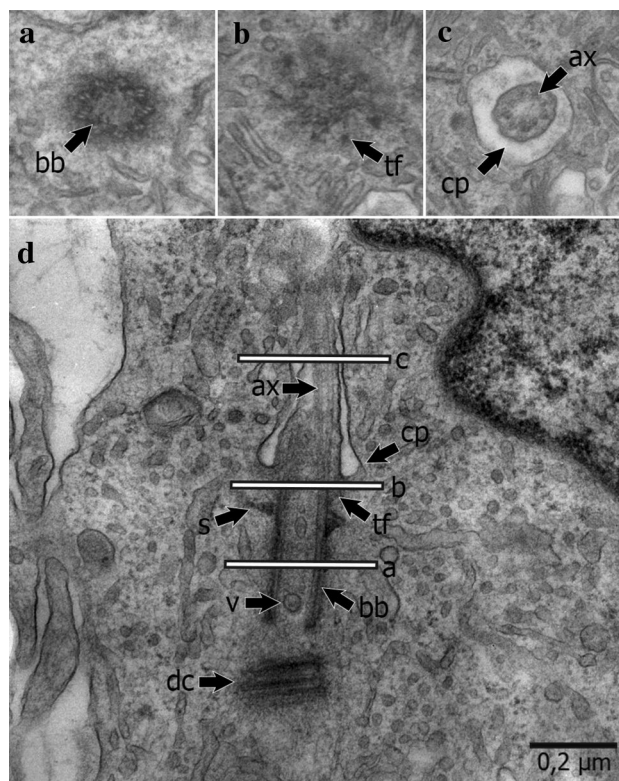
Fig. 3 TEM images showing primary cilia in GISTs. Primary cilia serial transversal sections in a GIST cell shows **a** basal body (bb), **b** transition zone characterised by the presence of transition fibres (tf) that anchors basal body to ciliary membrane and **c** axoneme (ax), that can be identified surrounded by the ciliary pocket (cp). **d** Longitudinal section of primary cilia in a GIST cell showing active vesicular trafficking (v) through the basal body (bb) and the different components of this organelle (*dc* daughter centriole; *s* satellites). White bars in **d** show the corresponding area in longitudinal view for transversal sections (**a–c**)

Furthermore, we tried to correlate Hh signalling activation with pathology grades of GIST (Table 1). Thus, we semi-quantitatively evaluated nuclear and cytoplasmic expression of Gli1. We found that low-grade GIST showed predominant cytoplasmic expression of Gli1 while main nuclear Gli1 staining was detected in high-grade tumours. These results suggest that Hh activation (evidenced by Gli1 nuclear expression) is especially present in high-grade GISTs.

Discussion

Primary cilia have been previously described in GISTs and their progenitor cells, ICCs [28–31]. According to the results provided in this study, primary cilium is confirmed to be a common and remarkable feature of GIST cells and not an incidental finding. Nevertheless, the exact role of this organelle in GIST remains unknown.

Primary cilia have been involved in cancer through different signalling pathways and mechanisms [32]. However, there is no agreement about the primary cilia number being increased or reduced in this pathology [33, 34]. One of the most studied ways of its implication in cancer development and maintenance is through Hh signalling pathway. This cellular signalling pathway disruption promotes several types of cancer, both in a ligand-dependent and -independent way, likely by maintaining cancer stem cells [20, 21]. It has been demonstrated that primary cilia play a vital role in physiological Hh signalling pathway, regulating the trafficking of different pathway components across the transition zone [24]. Furthermore, primary cilia are also important
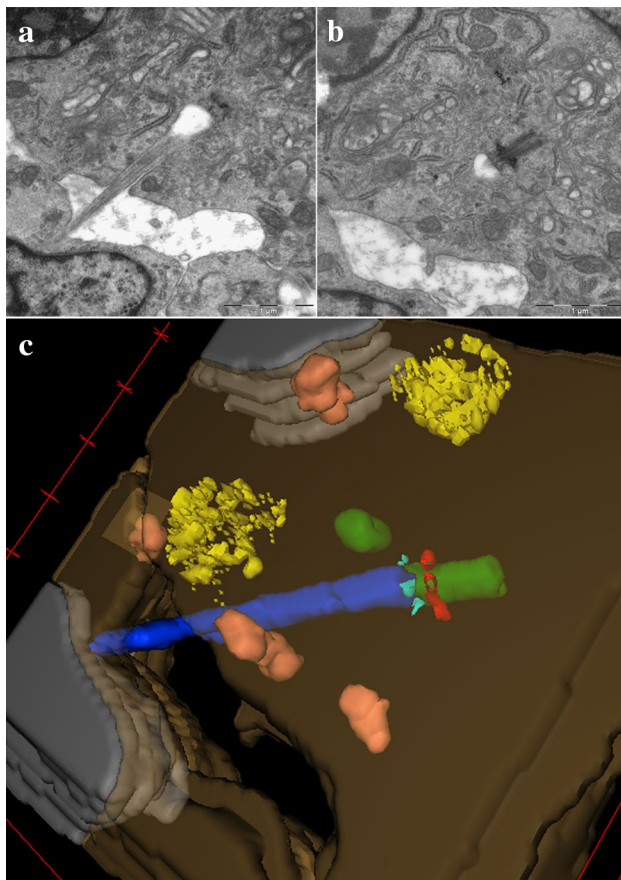
Fig. 4 Primary cilia 3-D reconstruction from TEM serial sections. **a**, **b** Two different serial images from a primary cilium in a GIST cell protruding into the cytoplasm of the neighbour cell. **c** Image corresponding to 3-D reconstruction. Primary cilia components are represented: the axoneme protruding out of the cell (blue), the basal body and the daughter centriole (green), satellites around basal body (red) and transition fibres that anchor the basal body to the ciliary pocket (cyan). Other organelles such as the Golgi apparatus (yellow) and some mitochondria (pink) are also shown. Nuclei are in grey and cytoplasm in clear brown

in cancer-related Hh signalling pathway. Thus, it has been shown that they are able to both, enhance or repress Hh ligand-independent tumorigenesis in models of medulloblastoma and basal cell carcinoma depending on the nature of the oncogenic signal [35, 36]. Moreover, a recent study has shown that epithelial–mesenchymal transition, an essential process in cancer progression and metastasis, induces ciliogenesis and Hh signalling pathway activation in in vitro models of breast cancer [37].

Nevertheless, the role of this signalling pathway in GIST remains unclear and its relation with primary cilia in these mesenchymal tumours has not been previously described.

Hh signalling pathway components have been reported to be expressed in human GIST by immunohistochemistry [25], RT-PCR and microarray analyses [26]. Furthermore, Tang et al. [26] showed, through microarrays analyses, Hh signalling pathway components and primary cilia-related proteins overexpression in GIST (independently of *KIT* or *PDGFR* mutations) compared to ICC. Furthermore, Shh agonists have been showed to increase cell proliferation in GIST cultures [38]. The results provided here confirm the presence of Hh signalling pathway components Gli1, Smo and Patched in GIST cells and their co-localisation with primary cilia.

Regarding the relation of Hh signalling pathway and KIT, the activating forms of Gli (Gli1 and Gli2) positively regulate KIT expression. Thus, pharmacological inhibition of Gli1 and Gli2 has been shown to reduce KIT expression and cell viability in GIST cell culture [26, 39]. As a counterpart, the repressor form Gli3 has been inversely correlated with KIT and its overexpression shown to reduce KIT expression [26, 40]. This effect was also present in wild-type GIST (non-*KIT*/non-*PDGFR* mutant GIST), suggesting that Hh signalling pathway activation and consequent Gli3 degradation may suppose a possible way to KIT overexpression in these tumours. Tang et al. [26] proposed that Hh signalling pathway would be ligand-independent; however, our results show that Patched is removed from ciliary axoneme, suggestive of ligand binding to Patched. Moreover, TEM images and 3D reconstructions show primary cilia in direct contact with surrounding cells. Hence, we propose that paracrine communication between GIST cells through primary cilia may be pivotal in Hh signalling pathway. This conclusion would agree with previously published results [25], where most GISTs expressing Hh signalling pathway components, expressed the Hh ligand Shh.

Further evidence of connection between GIST and Hh signalling pathway was proposed by Pelczar et al. [41]. Their studies defined *PDGFR*-positive GIST-like tumours in a Patched1-inactivated mutant murine model. However, both origin and tumour cells did not express KIT, so their classification as GIST may be doubtful. Besides, they did not perform ANO1 immunohistochemical assays (which is positive for up to one third of KIT-negative GIST [8]) that would have made results interpretation easier.

Here, we show evidence of the relation of Hh signalling pathway and primary cilia in human GISTs for the first time. Thus, we have shown that primary cilium is a relevant organelle in GIST cells, where it mediates Hh signalling pathway activation (likely in a ligand-dependent manner). Thus, ciliated cells showed Patched removal from axoneme, Smo expression and Gli1 entrance to cell nuclei, where
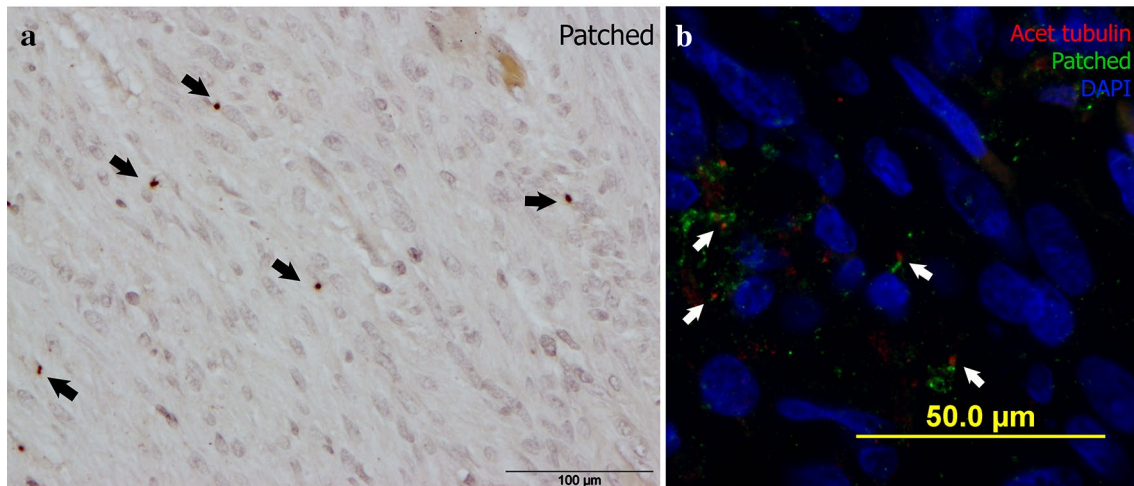
Fig. 5 Immunolabelling for Patched and its relation with primary cilia. **a** Punctiform Patched staining is located near nuclei (arrows). **b** Co-localisation of Acetylated-tubulin (labelling primary cilia axoneme; red) and Patched (green). Patched is not located in axoneme but in basal body (arrows), suggesting that Patched has been bound by the ligand and internalised out from the axoneme membrane
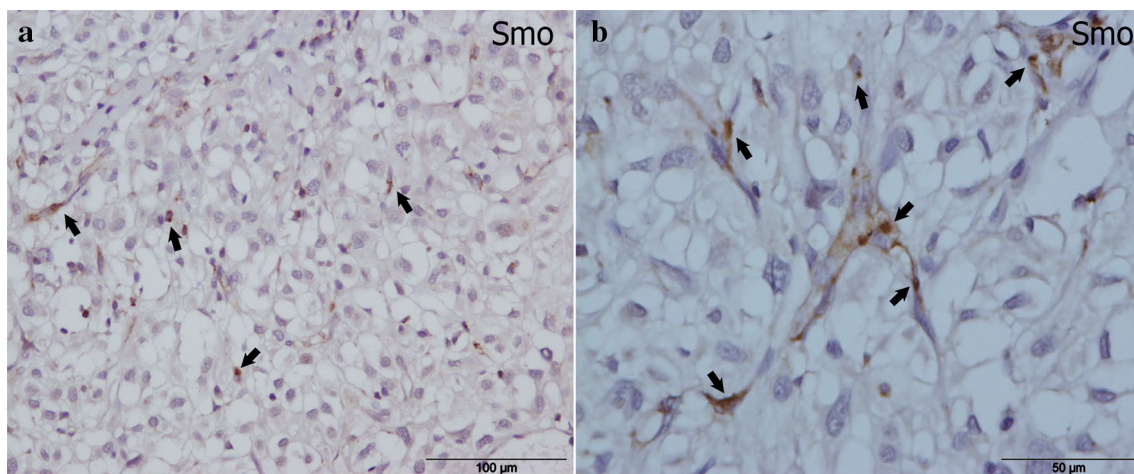
Fig. 6 Immunohistochemistry for Smo. **a** Panoramic view showing GIST cells expressing Smo in precise cell membrane regions and near nuclei (arrows). **b** Detail of immunostaining pattern

transcription of target genes is switched on. Moreover, 3D reconstructions and TEM images give an indisputable idea of the disposition and components of primary cilia, which sometimes are close or in direct contact with neighbour cells, likely mediating paracrine communication between tumor cells.
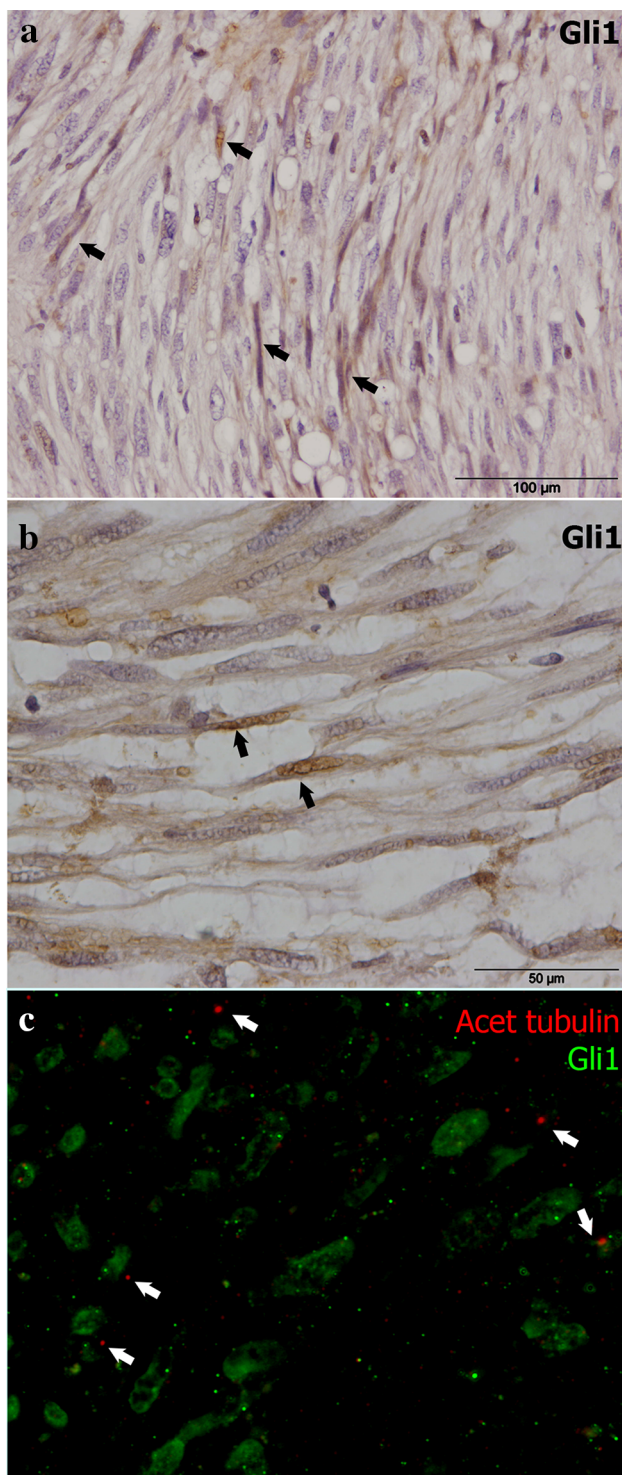
Fig. 7 Immunostaining for Gli1. Gli1-positive cells were heterogeneously presented in GISTs. Cytoplasmic and nuclear staining was detected. The presence of Gli1 in nuclei (arrows) means that Hh pathway is activated. **a** Magnification ×200. **b** Magnification ×400. **c** Co-localisation of Acetylated-tubulin (axoneme marker, in red) and Gli1 (green). Cells co-express a nuclear pattern of Gli1 and primary cilia (arrows) showing a clear relation between this organelle and the Hh signalling pathway activation

Table 1 Relation between Gli1 staining pattern and GIST grade

Case number	Grade	Nuclear staining	Cyto-plasmic staining
1	Low	+	++
2	Low	+	++
3	Low	+	+++
4	Low	++	+
5	High	++	++
6	High	++	+
7	High	+++	++
8	High	+	+

Low-grade tumours show a weaker nuclear staining than high-grade tumours while cytoplasmic staining was more intense in low-grade tumours. + weak expression, ++ moderate expression, +++ intense expression

Compliance with ethical standards

References

1. Zhao X, Yue C. Gastrointestinal stromal tumor. J Gastrointest Oncol. 2012;3:189–208. https://doi.org/10.3978/j.issn.2078-6891.2012.031.
2. Foo WC, Liegl-Atzwanger B, Lazar AJ. Pathology of gastrointestinal stromal tumors. Clin Med Insights Pathol. 2012;5:23–33.
3. Hirota S, Isozaki K, Moriyama Y, Hashimoto K, Nishida T, Ishiguro S. Gain-of-function mutations of c-kit in human gastrointestinal stromal tumors. Science (80-). 1998;279:577–80. https://doi.org/10.1126/science.279.5350.577.
4. Kindblom LG, Remotti HE, Aldenborg F, Meis-Kindblom JM. Gastrointestinal pacemaker cell tumor (GIPACT): gastrointestinal stromal tumors show phenotypic characteristics of the interstitial cells of Cajal. Am J Pathol. 1998;152:1259–69.
5. Niinuma T, Suzuki H, Sugai T. Molecular characterization and pathogenesis of gastrointestinal stromal tumor. Transl Gastroenterol Hepatol. 2018. https://doi.org/10.21037/tgh.2018.01.02.
6. Miettinen M, Wang ZF, Lasota J. DOG1 antibody in the differential diagnosis of gastrointestinal stromal tumors: a study of 1840 cases. Am J Surg Pathol. 2009;33:1401–8. https://doi.org/10.1097/PAS.0b013e3181a90e1a.
7. West RB, Corless CL, Chen X, et al. The novel marker, DOG1, is expressed ubiquitously in gastrointestinal stromal tumors irrespective of KIT or PDGFRA mutation status. Am J Pathol. 2004;165:107–13. https://doi.org/10.1016/S0002-9440(10)63279-8.

8. Liegl B, Hornick JL, Corless CL, Fletcher CDM. Monoclonal antibody DOG1.1 Shows higher sensitivity than KIT in the diagnosis of gastrointestinal stromal tumors, including unusual subtypes. Am J Surg Pathol. 2009;33:437–46. https://doi.org/10.1097/PAS.0b013e318186b158.

9. Güler B, lmaz F, Tokuç B, et al. Histopathological features of gastrointestinal stromal tumors and the contribution of DOG1 expression to the diagnosis. Balkan Med J. 2015;32:388–96. https://doi.org/10.5152/balkanmedj.2015.15912.

10. Stanich JE, Gibbons SJ, Eisenman ST, et al. Ano1 as a regulator of proliferation. Am J Physiol Liver Physiol. 2011;301:G1044–G10511051. https://doi.org/10.1152/ajpgi.00196.2011.

11. Ruppersburg CC, Hartzell HC. The Ca2+-activated Cl- channel ANO1/TMEM16A regulates primary ciliogenesis. Mol Biol Cell. 2014;25:1793–807. https://doi.org/10.1091/mbc.E13-10-0599.

12. Simon S, Grabellus F, Ferrera L, et al. DOG1 regulates growth and IGFBP5 in gastrointestinal stromal tumors. Cancer Res. 2013;73:3661–700. https://doi.org/10.1158/0008-5472.CAN-12-3839.

13. Berglund E, Akcakaya P, Berglund D, et al. Functional role of the Ca^{2+}-activated Cl^- channel DOG1/TMEM16A in gastrointestinal stromal tumor cells. Exp Cell Res. 2014;326:315–25. https://doi.org/10.1016/j.yexcr.2014.05.003.

14. Malicki JJ, Johnson CA. The cilium: cellular antenna and central processing unit. Trends Cell Biol. 2017;27:126–40. https://doi.org/10.1016/j.tcb.2016.08.002.

15. Garcia-Gonzalo FR, Reiter JF. Open sesame: how transition fibers and the transition zone control ciliary composition. Cold Spring Harb Perspect Biol. 2017. https://doi.org/10.1101/cshperspect.a028134.

16. Braun DA, Hildebrandt F. Ciliopathies. Cold Spring Harb Perspect Biol. 2017. https://doi.org/10.1101/cshperspect.a028191.

17. Pala R, Alomari N, Nauli SM. Primary cilium-dependent signaling mechanisms. Int J Mol Sci. 2017. https://doi.org/10.3390/ijms18112272.

18. Wheway G, Nazlamova L, Hancock JT. Signaling through the primary cilium. Front Cell Dev Biol. 2018;6:1–13. https://doi.org/10.3389/fcell.2018.00008.

19. Mitchison HM, Valente EM. Motile and non-motile cilia in human pathology: from function to phenotypes. J Pathol. 2017;241:294–309. https://doi.org/10.1002/path.4843.

20. Amakye D, Jagani Z, Dorsch M. Unraveling the therapeutic potential of the Hedgehog pathway in cancer. Nat Med. 2013;19:1410–22. https://doi.org/10.1038/nm.3389.

21. Chahal KK, Parle M, Abagyan R. Hedgehog pathway and smoothened inhibitors in cancer therapies. Anticancer Drugs. 2018. https://doi.org/10.1097/CAD.0000000000000609.

22. Scales SJ, De Sauvage FJ. Mechanisms of Hedgehog pathway activation in cancer and implications for therapy. Trends Pharmacol Sci. 2009. https://doi.org/10.1016/j.tips.2009.03.007.

23. Ramsbottom SA, Pownall ME, Roelink H, Conway SJ, Europe PMC Funders Group. Regulation of hedgehog signalling inside and outside the cell. J Dev Biol. 2016. https://doi.org/10.3390/jdb4030023.

24. Rohatgi R, Milenkovic L, Scott MP. Patched1 regulates hedgehog signaling at the primary cilium. Science (80-). 2007;317:372–6. https://doi.org/10.1126/science.1139740.

25. Yoshizaki A, Nakayama T, Naito S, et al. Expressions of sonic hedgehog, patched, smoothened and Gli-1 in human intestinal stromal tumors and their correlation with prognosis. World J Gastroenterol. 2006;12:5687–91.

26. Tang C-M, Lee TE, Syed SA, et al. Hedgehog pathway dysregulation contributes to the pathogenesis of human gastrointestinal stromal tumors via GLI-mediated activation of KIT expression. Oncotarget. 2016;7:78226–41.

27. Schindelin J, Arganda-Carreras I, Frise E, et al. Fiji: an open-source platform for biological-image analysis. Nat Methods. 2012;9:676–82. https://doi.org/10.1038/nmeth.2019.

28. Castiella T, Muñoz G, Luesma MJ, et al. Primary cilia in gastric gastrointestinal stromal tumours (GISTs): an ultrastructural study. J Cell Mol Med. 2013;17:844–53. https://doi.org/10.1111/jcmm.12067.

29. Dvorak J, Sitorova V, Nikolov DH, et al. Primary cilia in gastrointestinal stromal tumors. Neoplasma. 2014;61:305–8. https://doi.org/10.4149/neo_2014_039.

30. Junquera C, Cantarero I, Luesma MJ, et al. The primary cilium: a relevant characteristic in interstitial cells of rat duodenum enteric plexus. Histol Histopathol. 2011;26:461–70.

31. Junquera C, Castiella T, Muñoz G, et al. Biogenesis of a new type of extracellular vesicles in gastrointestinal stromal tumors: ultrastructural profiles of spheresomes. Histochem Cell Biol. 2016;146:557–67. https://doi.org/10.1007/s00418-016-1460-5.

32. Seeger-Nukpezah T, Little JL, Serzhanova V, Golemis EA. Cilia and cilia-associated proteins in cancer. Drug Discov Today Dis Mech. 2013;10:e135–e142142. https://doi.org/10.1016/j.ddmec.2013.03.004.

33. Yasar B, Linton K, Slater C, Byers R. Primary cilia are increased in number and demonstrate structural abnormalities in human cancer. J Clin Pathol. 2016;52:286–8. https://doi.org/10.1136/jclinpath.

34. Hassounah NB, Nagle R, Saboda K, et al. Primary cilia are lost in preinvasive and invasive prostate cancer. PLoS ONE. 2013;8:1–19. https://doi.org/10.1371/journal.pone.0068521.

35. Han YG, Kim HJ, Dlugosz AA, et al. Dual and opposing roles of primary cilia in medulloblastoma development. Nat Med. 2009;15:1062–5. https://doi.org/10.1038/nm.2020.

36. Wong SY, Seol AD, So PL, et al. Primary cilia can both mediate and suppress Hedgehog pathway-dependent tumorigenesis. Nat Med. 2009;15:1055–61. https://doi.org/10.1038/nm.2011.

37. Guen VJ, Chavarria TE, Kröger C, et al. EMT programs promote basal mammary stem cell and tumor-initiating cell stemness by inducing primary ciliogenesis and Hedgehog signaling. Proc Natl Acad Sci. 2017. https://doi.org/10.1073/pnas.1711534114.

38. Qi Y, Zhao W, Wang Z, et al. Cross regulation of signaling pathways in gastrointestinal stromal tumor. Oncol Lett. 2018;16:6770–6. https://doi.org/10.3892/ol.2018.9494.

39. Saponara M, Urbini M, Astolfi A, et al. Molecular characterization of metastatic exon 11 mutant gastrointestinal stromal tumors (GIST) beyond KIT/PDGFRalpha genotype evaluated by next generation sequencing (NGS). Oncotarget. 2015;6:1–15. https://doi.org/10.18632/oncotarget.6278.

40. Cain JE, Islam E, Haxho F, et al. GLI3 repressor controls functional development of the mouse ureter. J Clin Investig. 2011;121:1199–206. https://doi.org/10.1172/JCI45523.

41. Pelczar P, Zibat A, Van Dop WA, et al. Inactivation of patched1 in mice leads to development of gastrointestinal stromal-like tumors that express Pdgfr but not kit. Gastroenterology. 2013;144:134–44. https://doi.org/10.1053/j.gastro.2012.09.061.